Many-body theory of spin-current driven instabilities in magnetic insulators

Roberto E. Troncoso,[1,2,*] Arne Brataas,[1] and Rembert A. Duine[2,3]

[1]*Center for Quantum Spintronics, Department of Physics, Norwegian University of Science and Technology, NO-7491 Trondheim, Norway*

[2]*Institute for Theoretical Physics and Center for Extreme Matter and Emergent Phenomena, Utrecht University, Leuvenlaan 4, 3584 CE Utrecht, The Netherlands*

[3]*Department of Applied Physics, Eindhoven University of Technology, P.O. Box 513, 5600 MB Eindhoven, The Netherlands*

(Received 23 September 2018; revised manuscript received 8 March 2019; published 22 March 2019)

We consider a magnetic insulator in contact with a normal metal. We derive a self-consistent Keldysh effective action for the magnon gas that contains the effects of magnon-magnon interactions and contact with the metal to lowest order. Self-consistent expressions for the dispersion relation, temperature, and chemical potential for magnons are derived. Based on this effective action, we study instabilities of the magnon gas that arise due to spin current flowing across the interface between the normal metal and the magnetic insulator. We find that the stability phase diagram is modified by an interference between magnon-magnon interactions and interfacial magnon-electron coupling. These effects persist at low temperatures and for thin magnetic insulators.

DOI: 10.1103/PhysRevB.99.104426

I. INTRODUCTION

Understanding the interplay between magnetization dynamics and spin currents is a fundamental issue that is relevant for spintronic devices [1–4]. In particular, there is a growing interest, both theoretically [5–13] and experimentally [14–20], in magnetic insulators such as yttrium iron garnet (YIG) in contact with heavy metals like Pt (YIG|Pt bilayers). In these hybrid systems, magnons and magnetization dynamics are excited via interfacial spin-transfer torques [21,22]. The realization of a Bose-Einstein condensate (BEC) of magnons through this mechanism has recently been proposed [23]. Auto-oscillations driven by the spin Hall effect [24] and thermal spin current [25,26] have very recently been observed. Earlier, a condensate has been realized at room temperature in YIG by other means, namely via parametric pumping [27]. This is an example of a nonequilibrium condensate of quasiparticles [28–34]. Such nonequilibrium BECs have attracted a great deal of attention and occur in different physical systems such as excitons [35–37], phonons [38], polaritons [39], and photons [40]. Specifically, condensation of magnons has stimulated efforts to control coherent transport of spin waves at room temperature [41].

In this paper, we present a microscopic study of magnon instabilities (such as Bose-Einstein condensation and/or swasing [42]) in insulating ferromagnets (F) induced via spin-current injection through the interface with an adjacent normal metal (M; see Fig. 1). The interfacial spin current is generated by the combined effects of a thermal gradient across the interface [7,43] and the spin Hall effect in the normal metal (leading to a spin accumulation in the normal metal at the interface). We derive a Keldysh effective action for the magnons in the F up to second order in the coupling with the normal metal. Through this approach, self-consistent relations are derived for the thermodynamic variables and the dispersion relation of magnons. We use this description to find the stability phase diagram. Besides introducing a different theoretical framework, this approach improves the previous treatment [42] by including interference effects between magnon-magnon interactions and interfacial magnon-electron coupling. These effects are finite at low temperature, and may prevent instabilities if they are very strong.

The remainder of this article is organized as follows. The following Sec. II introduces our model to describe the magnon dynamics and its coupling to electrons. In Sec. III, we proceed to derive the effective action for the magnons within the functional formulation of the Schwinger-Keldysh formalism. In Sec. IV, we construct the stability phase diagram. We end in Sec. V by summarizing our results with a brief discussion and conclusion. In the Appendixes, we detail various technical steps of the calculations.

II. MODEL

The system under consideration is a F in contact with a M as is displayed in Fig. 1. We assume a three-dimensional system of localized spins in quasiequilibrium at temperature T_m and magnon chemical potential μ_m [44,45]. The normal metal is at temperature T_e and has a spin accumulation $\Delta\mu$.

The spin Hamiltonian is introduced by labeling the square lattice site by the position $\mathbf{x}$, with the spin operator $\hat{\mathbf{S}}_{\mathbf{x}}$ at position $\mathbf{x}$. The nearest-neighbor Hamiltonian is

$$\hat{\mathcal{H}}_{\mathrm{S}} = -J_e \sum_{\langle \mathbf{x},\mathbf{x}' \rangle} \hat{\mathbf{S}}_{\mathbf{x}} \cdot \hat{\mathbf{S}}_{\mathbf{x}'} - B \sum_{\mathbf{x}} \hat{S}^z_{\mathbf{x}} + \frac{K_z}{2} \sum_{\mathbf{x}} \left(\hat{S}^z_{\mathbf{x}}\right)^2, \qquad (1)$$

where $J_e > 0$ is the exchange coupling between nearest neighbors, K_z is an easy-plane anisotropy constant, and B is the external magnetic field in units of energy. We consider linearized spin excitations, magnons, around the z direction for sufficiently large fields. These are introduced by the

*r.troncoso@ntnu.no

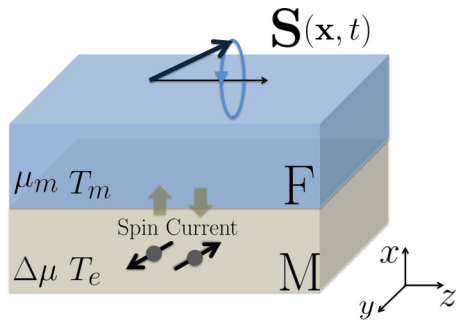

FIG. 1. Schematic illustration of spin-transfer induced spin-wave excitations of the insulating magnetic film in contact with a normal metal ($F|M$). A spin accumulation $\Delta\mu$ is induced in the metal via the spin Hall effect. The magnons are assumed to be in quasiequilibrium with a chemical potential μ_m. In turn, the spin accumulation exerts a torque on the magnetization in F. A temperature gradient $T_m - T_e$, applied longitudinally also contributes to the net spin-current flow through the interface.

Holstein-Primakoff transformation [46–48] that quantizes the spins in terms of bosons, $\hat{S}^+_{\mathbf{x}} = \sqrt{2S - \hat{b}^\dagger_{\mathbf{x}}\hat{b}_{\mathbf{x}}}\,\hat{b}_{\mathbf{x}}$, $\hat{S}^-_{\mathbf{x}} = \hat{b}^\dagger_{\mathbf{x}}\sqrt{2S - \hat{b}^\dagger_{\mathbf{x}}\hat{b}_{\mathbf{x}}}$ and $\hat{S}^z_{\mathbf{x}} = (S - \hat{b}^\dagger_{\mathbf{x}}\hat{b}_{\mathbf{x}})$ with S the spin quantum number. One magnon, created (annihilated) at site $\mathbf{x}$ of the lattice by the operator $\hat{b}^\dagger_{\mathbf{x}}(\hat{b}_{\mathbf{x}})$, corresponds to changing the total spin with $+\hbar(-\hbar)$. Expanding up to fourth order in the magnon operators, the spin Hamiltonian becomes $\hat{\mathcal{H}}_S \simeq \hat{\mathcal{H}}^{(2)}_S + \hat{\mathcal{H}}^{(4)}_S$, where terms up to order $1/\sqrt{S}$ are kept. In momentum space the quadratic part of the Hamiltonian is given by

$$\hat{\mathcal{H}}^{(2)}_S = \sum_{\mathbf{q}} \epsilon_{\mathbf{q}} \hat{b}^\dagger_{\mathbf{q}} \hat{b}_{\mathbf{q}}. \tag{2}$$

In the long-wavelength limit, the magnon dispersion is $\epsilon_{\mathbf{q}} = Aq^2 + \epsilon_0$, where $\epsilon_0 = B - SK_z$ is the magnon gap and $A = 3SJ_e a^2$ is the spin stiffness with a the lattice spacing. Furthermore,

$$\hat{\mathcal{H}}^{(4)}_S = \sum_{\mathbf{q}_1,\mathbf{q}_2,\mathbf{q}_3,\mathbf{q}_4} V^{(2,2)}_{\mathbf{q}_1,\mathbf{q}_2,\mathbf{q}_3,\mathbf{q}_4} \hat{b}^\dagger_{\mathbf{q}_1} \hat{b}^\dagger_{\mathbf{q}_2} \hat{b}_{\mathbf{q}_3} \hat{b}_{\mathbf{q}_4}, \tag{3}$$

where momentum conservation is implicit in $V^{(2,2)}$. This part of the Hamiltonian represents magnon-magnon interactions that result from exchange and anisotropy that causes the thermalization of magnons in the F [47]. In the long-wavelength limit the interaction between magnons is dominated by the anisotropy energy. Henceforth we consider magnons with sufficiently long wavelengths since we are interested in long-wavelength instabilities in the F. Thus we approximate the scattering amplitude by $V^{(2,2)}_{\mathbf{q}_1,\mathbf{q}_2,\mathbf{q}_3,\mathbf{q}_4} = (K_z/2N)\delta_{\mathbf{q}_1+\mathbf{q}_2-\mathbf{q}_3-\mathbf{q}_4}$, with N the total number of spins. The exact result containing contributions from the exchange interactions is found in Appendix A.

The electronic degrees of freedom in the metal are described by the tight-binding Hamiltonian

$$\hat{\mathcal{H}}_e = -t \sum_{\langle \mathbf{x},\mathbf{x}'\rangle,\sigma} \hat{\psi}^\dagger_{\mathbf{x},\sigma} \hat{\psi}_{\mathbf{x}',\sigma} - \sum_{\mathbf{x},\sigma} \mu_\sigma \hat{\psi}^\dagger_{\mathbf{x},\sigma} \hat{\psi}_{\mathbf{x},\sigma}, \tag{4}$$

in terms of second-quantized operators $\hat{\psi}^\dagger_{\mathbf{x},\sigma}(\hat{\psi}_{\mathbf{x},\sigma})$ that create (annihilate) an electron at site $\mathbf{x}$ in M with spin σ. The hopping amplitude is t and the spin-dependent chemical potential is μ_σ. The latter results from the spin Hall effect in the M and defines a nonzero spin accumulation $\Delta\mu = \mu_\uparrow - \mu_\downarrow$.

We assume the magnons and electrons predominantly interact via an exchange coupling between the spin density of electrons and localized magnetic moments facing the $F|M$ interface. The Hamiltonian that couples metal and insulator is $\hat{\mathcal{H}}_{e-m} = -\sum_{\mathbf{x},\mathbf{x}'} J_{\mathbf{x}\mathbf{x}'} \hat{\mathbf{S}}_{\mathbf{x}} \cdot \hat{\mathbf{s}}_{\mathbf{x}'}$, where $J_{\mathbf{x}\mathbf{x}'}$ is the coupling strength that depends on the interface details. The spin density of electrons at site $\mathbf{x}$ is $\hat{\mathbf{s}}_{\mathbf{x}} = \sum_{\sigma,\sigma'} \hat{\psi}^\dagger_{\mathbf{x},\sigma} \boldsymbol{\tau}_{\sigma\sigma'} \hat{\psi}_{\mathbf{x},\sigma'}$, with $\boldsymbol{\tau}$ the Pauli matrix vector. After the Holstein-Primakoff transformation on the spins in the insulator, the electron-magnon Hamiltonian is

$$\hat{\mathcal{H}}_{e-m} = -\sum_{\mathbf{x},\mathbf{x}'} J_{\mathbf{x}\mathbf{x}'} [\sqrt{2S}(\hat{b}^\dagger_{\mathbf{x}} \hat{\psi}^\dagger_{\mathbf{x}',\downarrow} \hat{\psi}_{\mathbf{x}',\uparrow} + \text{H.c.}) + (S - \hat{b}^\dagger_{\mathbf{x}} \hat{b}_{\mathbf{x}})(\hat{\psi}^\dagger_{\mathbf{x}',\uparrow} \hat{\psi}_{\mathbf{x}',\uparrow} - \hat{\psi}^\dagger_{\mathbf{x}',\downarrow} \hat{\psi}_{\mathbf{x}',\downarrow})], \tag{5}$$

up to quadratic order in the magnon operators. Hence, when an electron flips its spin at the interface it creates (or annihilates) one magnon in the insulating F [5,6]. The electron-magnon interaction has been studied in various related contexts [13,49–54]. Its evaluation through the self-energy has been useful for the study of magnetic damping and noise [55], magnon-induced superconductivity [56], and spin transport [57]. In our work we go further by studying, in combination magnon-magnon interactions, its effect on the single-magnon energy. Additionally, thermodynamic properties like temperature and chemical potential of the magnon gas are computed self-consistently with the electron-magnon coupling as the perturbative parameter.

III. NONEQUILIBRIUM THEORY

In this section, we derive an effective action for the magnon gas using a functional Keldysh approach [58]. We also calculate the self-energy that magnons acquire by their interaction with the electrons.

A. Self-energy due to electron-magnon coupling

The starting point is the functional integral

$$\mathcal{Z} = \int \mathcal{D}\phi^* \mathcal{D}\phi \mathcal{D}\psi^* \mathcal{D}\psi \exp\left\{\frac{i}{\hbar}\mathcal{S}[\psi, \psi^*, \phi, \phi^*]\right\}. \tag{6}$$

The action is expressed in terms of bosonic fields $\phi_{\mathbf{x}}(t)$, describing magnons, and fermionic fields $\psi_{\mathbf{x},\sigma}(t)$, describing electrons. Thus,

$$\mathcal{S}[\psi, \psi^*, \phi, \phi^*] = \mathcal{S}_0[\phi, \phi^*] + \int_{\mathcal{C}^\infty} dt dt' \sum_{\mathbf{x}\mathbf{x}'} \sum_{\sigma\sigma'} \psi^*_{\mathbf{x},\sigma}(t) \times \mathcal{K}^{\mathbf{x}\mathbf{x}'}_{\sigma\sigma'}(t,t') \psi_{\mathbf{x}',\sigma'}(t'), \tag{7}$$

with $\mathcal{S}_0[\phi, \phi^*] = \int_{\mathcal{C}^\infty} dt [\int d\mathbf{x} \phi^* i\hbar\partial_t \phi - \mathcal{H}_S[\phi, \phi^*]]$, the action for magnons uncoupled with the electrons. The magnon Hamiltonian is in the continuum limit given by

$$\mathcal{H}_S[\phi, \phi^*] = \int d\mathbf{x} \phi^* \left(-A\nabla^2 + \epsilon_0 + \frac{K_z}{2}|\phi|^2\right)\phi, \tag{8}$$

and follows directly from evaluating the Hamiltonian in Eqs. (2) and (3) for the bosonic fields and taking the

continuum limit. The time integration in Eq. (7) is over the Keldysh contour $\mathcal{C}^\infty$, whereby the functional integral in Eq. (6) is over all fields $\phi_{\mathbf{x}}(t)$ and $\psi_{\mathbf{x},\sigma}(t)$ that evolve forward in time from $-\infty$ to t_0, and backwards from t_0 to $-\infty$. The kernel in Eq. (7) is defined as

$$\mathcal{K}^{\mathbf{x}\mathbf{x}'}_{\sigma\sigma'}(t,t') \equiv G^{-1}_{\mathbf{x}\mathbf{x}';\sigma\sigma'}(t,t')\delta(t,t') + \delta\mathcal{K}^{\mathbf{x}\mathbf{x}'}_{\sigma\sigma'}(t,t'), \quad (9)$$

where G^{-1} is the inverse of the free Green's function for the electrons that obeys

$$\sum_{\mathbf{x}''}\left[i\hbar\delta_{\mathbf{x}\mathbf{x}''}\frac{\partial}{\partial t} + \mathrm{t}_{\mathbf{x}\mathbf{x}'';\sigma}\right]G_{\mathbf{x}''\mathbf{x}';\sigma\sigma'}(t,t') = \hbar\delta(t,t')\delta_{\sigma\sigma'}\delta_{\mathbf{x}\mathbf{x}'}, \quad (10)$$

with $\mathrm{t}_{\mathbf{x}\mathbf{x}';\sigma} = [t(\delta_{\mathbf{x},\mathbf{x}'+\mathbf{1}} + \delta_{\mathbf{x},\mathbf{x}'-\mathbf{1}}) + \mu_\sigma\delta_{\mathbf{x}\mathbf{x}'}]$, where the notation $\pm\mathbf{1}$ denotes all next-nearest neighbors. The interactions between electronic spin and magnetic moments are described by

$$\delta\mathcal{K}^{\mathbf{x}\mathbf{x}'}_{\sigma\sigma'}(t,t') = \sqrt{2S}\delta_{\mathbf{x}\mathbf{x}'}\sum_{\mathbf{x}''}J_{\mathbf{x}''\mathbf{x}'}\left[\phi^*_{\mathbf{x}''}(t)\tau^+_{\sigma\sigma'} + \phi_{\mathbf{x}''}(t)\tau^-_{\sigma\sigma'} + \frac{1}{\sqrt{2S}}[S - \phi^*_{\mathbf{x}''}(t)\phi_{\mathbf{x}''}(t)]\tau^z_{\sigma\sigma'}\right]\delta(t,t'), \quad (11)$$

where $\tau^\pm = (\tau^x \pm i\tau^y)/2$.

We now integrate out the electronic degrees of freedom in Eq. (7). The functional integration can be done exactly since the fermionic part of the action is a Gaussian integral. This leads us to an effective theory for magnons in the F, $\mathcal{Z} = \int\mathcal{D}\phi^*\mathcal{D}\phi\exp\{i\mathcal{S}_\mathrm{m}[\phi^*,\phi]/\hbar\}$, where $\mathcal{S}_\mathrm{m}$ contains all the electronic information and its influence on the magnon dynamics. To second order in the electron-magnon coupling, the action is written as $\mathcal{S}_\mathrm{m} = \mathcal{S}_0 + i\mathrm{Tr}[G\delta\mathcal{K}] + i\mathrm{Tr}[G\delta\mathcal{K}G\delta\mathcal{K}]/2\hbar$, where the last two terms correspond to electron-magnon scattering processes that we describe below. For more details, please see Appendix B.

We are interested in the limit when the F is thin enough. In this case the spin waves only propagate parallel to the interface. In Fourier space the action simplifies to

$$\mathcal{S}_\mathrm{m} = \mathcal{S}_0 - \int_{\mathcal{C}^\infty}dtdt'\int\frac{d\mathbf{q}}{(2\pi)^2}\phi^*_{\mathbf{q}}(t)\hbar\Sigma_{\mathrm{st};\mathbf{q}}(t,t')\phi_{\mathbf{q}}(t'), \quad (12)$$

where $\mathbf{q}$ is the in-plane wave vector. The self-energy is denoted as $\hbar\Sigma_\mathrm{st}$ and describes processes that dress the magnons due to the electron-magnon coupling; see the Feynman diagrams in Fig. 2. The self-energy is given (in real space) by

$$\hbar\Sigma_{\mathrm{st};\mathbf{x}\mathbf{x}'}(t,t') = 2S\sum_{\mathbf{x}_1\mathbf{x}_2}J_{\mathbf{x}\mathbf{x}_1}J_{\mathbf{x}'\mathbf{x}_2}\Pi^{\uparrow\downarrow}_{\mathbf{x}_1\mathbf{x}_2}(t,t') - \delta_{\mathbf{x}\mathbf{x}'}\delta(t,t')\sum_{\mathbf{x}_1}J_{\mathbf{x}_1\mathbf{x}'}\delta\bar{n}(\mathbf{x}_1,t), \quad (13)$$

where the electron bubble reads $\Pi^{\sigma\sigma'}_{\mathbf{x}\mathbf{x}'}(t,t') = -\frac{i}{\hbar}G_{\mathbf{x}\mathbf{x}';\sigma}(t,t')G_{\mathbf{x}'\mathbf{x};\sigma'}(t',t)$, which contains the information of the electronic quasiparticles in the M. The first term on the right-hand side accounts for the creation and annihilation of magnons by means of a spin-flip process; see Fig. 2(a), while the second term describes a field produced by an unbalanced electronic density at the interface; see Fig. 2(b). This imbalance is defined by $\delta\bar{n} = \bar{n}_\uparrow - \bar{n}_\downarrow$, where $\bar{n}_\sigma(\mathbf{x}_1) = n_\sigma - S\sum_{\mathbf{x}_2\mathbf{x}_3}\int_{\mathcal{C}^\infty}dt'J_{\mathbf{x}_3\mathbf{x}_2}\Pi^{\sigma\sigma}_{\mathbf{x}_1\mathbf{x}_2}(t,t')\tau^z_{\sigma\sigma}$.

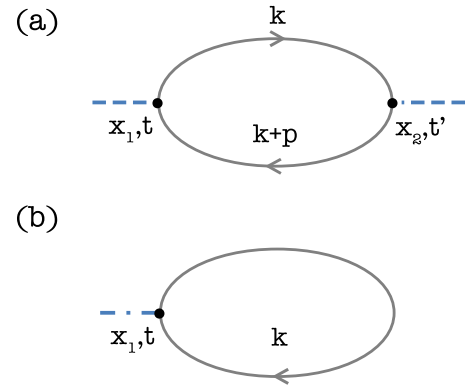

FIG. 2. Feynman diagrams contributing to the magnon dynamics due to electron-magnon interactions at the $F|M$ interface. (a) Electron bubble diagram representing the annihilation and creation of magnons via spin-flip processes. (b) Diagram for the enhanced spin polarization. The momentum carried by the magnon is denoted by $\mathbf{p}$.

The self-energy in Eq. (12) is written in momentum space where $\hbar\Sigma_{\mathrm{st};\mathbf{q}} = \sum_{k_\perp}\hbar\Sigma_{\mathrm{st};\mathbf{k}}$, with $\hbar\Sigma_{\mathrm{st};\mathbf{k}}$ being the Fourier transform of Eq. (13). The summation on $k_\perp$ represents a sum over all electronic wave vectors perpendicular to the interface. In order to find concrete results, we give expressions for the retarded/advanced component of the self-energy, $\hbar\Sigma^{(\pm)}_{\mathrm{st};\mathbf{x}\mathbf{x}'}(t,t') = 2S\sum_{\mathbf{x}_1\mathbf{x}_2}J_{\mathbf{x}\mathbf{x}_1}J_{\mathbf{x}'\mathbf{x}_2}\Pi^{\uparrow\downarrow,(\pm)}_{\mathbf{x}_1\mathbf{x}_2}(t,t')$, which we need later on. Details of its derivation are found in Appendix C. In addition, we assume that the interfacial exchange coupling is nonzero only at the $F|N$ interface, i.e., $J_{\mathbf{x}\mathbf{x}'} = J\delta_{\mathbf{x}\mathbf{x}'}\delta_{\mathbf{x}\mathbf{x}_0}$, with $\mathbf{x}_0$ the position of the interface. Thus the Fourier transform of the electron bubble, in energy and momentum space, is

$$\Pi^{\uparrow\downarrow,(\pm)}(\mathbf{k},\epsilon) = \frac{1}{2}N(0)a^3\left[\frac{1}{3}\left(\frac{\mathbf{k}}{2k_F}\right)^2 - 1\right] - \frac{N(0)a^3\epsilon\Delta\mu}{16\epsilon_F^2} \times\left[\left(\frac{2k_F}{\mathbf{k}}\right)^2 + 1\right] \pm i\frac{\pi N(0)a^3k_F}{8\epsilon_F|\mathbf{k}|}(\Delta\mu - \epsilon) \times\Theta\left[1 - \left(\frac{|\mathbf{k}|}{2k_F}\right)^2\right], \quad (14)$$

with $N(0)$ the electronic density of states at the Fermi level, and k_F and ϵ_F the Fermi wave number and energy, respectively. The Θ function represents the Heaviside step function.

B. Effective action

We are interested in real-time dynamics of the magnon gas, thus we expect the effective action to depend only on the retarded part of $\hbar\Sigma_{\mathrm{st};\mathbf{q}}(t,t')$. Moreover, since the magnon-magnon interactions resulting from the anisotropy are short ranged, we can use the so-called ladder approximation [58]. We project, in Eq. (12), the fields onto the real-time axis by the substitution $\phi_\pm = \Psi \pm \xi/2$, where momentum labels were omitted. Ψ represents the classical field and the symbol $\pm$ refers to the upper and lower branch of the Keldysh contour. The field ξ denotes the quantum fluctuations which by the

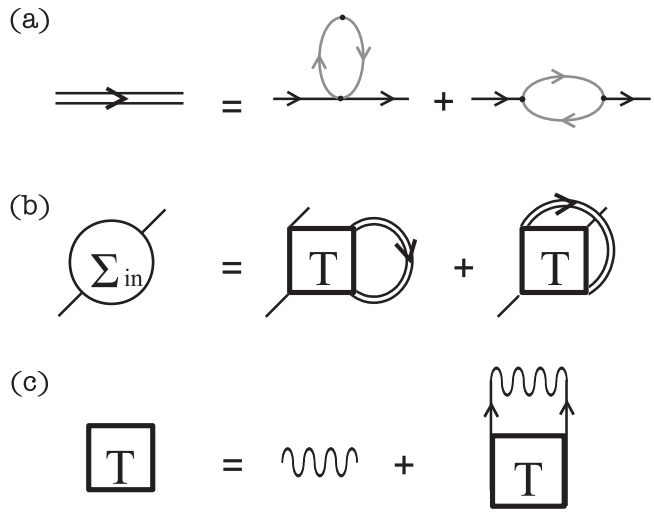

FIG. 3. (a) Feynman diagram for the dressed Green's function of magnons due to the coupling with the M. Bubble diagram represents the self-energy given in Eq. (13). (b) Diagrammatic representation for the interacting self-energy and (c) the T-matrix ladder approximation, where the wavy lines denote the contact interaction K_z. Note that the self-energy and T matrix are determined by the dressed and free propagators, respectively.

current purpose are disregarded. Details of this calculation are outlined in Appendix D. Following Ref. [58], we ultimately find a one-particle-irreducible long-wavelength effective action for the classical field Ψ that is given by

$$\mathcal{S}_{\rm eff}[\Psi,\Psi^*]=\int dt\int\frac{d\mathbf{q}}{(2\pi)^2}\Psi^*(\mathbf{q},t)\Big(i\hbar\frac{\partial}{\partial t}-\epsilon'(\mathbf{q})+\mu_m -a^2K_zn_{\rm th}-\frac{K_z}{2}|\Psi(\mathbf{q},t)|^2\Big)\Psi(\mathbf{q},t). \tag{15}$$

The single-particle dispersion relation of magnons is renormalized by the magnon-magnon interactions and the coupling with electrons, and obeying the self-consistent relation

$$\epsilon'(\mathbf{q})=\epsilon(\mathbf{q})+{\rm Re}[\hbar\Sigma^{(+)}(\mathbf{q};\epsilon'(\mathbf{q})-\mu_m)]. \tag{16}$$

Here, $\hbar\Sigma=\hbar\Sigma_{\rm st}+\hbar\Sigma_{\rm in}$ is the sum of contributions due to the coupling with electrons and magnon-magnon interactions, and μ_m is the chemical potential of magnons. Moreover, we have included in the action Eq. (15) a mean-field interaction with the thermal cloud of magnons, whose density is $n_{\rm th}=\zeta(3/2)d_F(k_BT_m/4\pi A)^{3/2}$, with $d_{\rm F}$ the thickness of F and ζ the Riemann zeta function. The derivation of $n_{\rm th}$ is straightforward and can be found in Ref. [59]. The self-energy $\hbar\Sigma_{\rm in}$ due to interactions is diagrammatically shown in Fig. 3. The real part of $\hbar\Sigma_{\rm in}$—which we need later on—reads

$${\rm Re}[\hbar\Sigma^{(+)}_{\rm in}(\mathbf{0},\epsilon_0-\mu_m)]=-a^2K_z\int\frac{d\mathbf{q}'}{(2\pi)^2}\int\frac{d\epsilon'}{(2\pi)}N_B\Big(\frac{\epsilon'-\Delta\mu}{k_BT_e}\Big)\frac{{\rm Im}[\hbar\Sigma^{(+)}_{\rm st}(\mathbf{q}',\epsilon')]}{[\epsilon'-\epsilon(\mathbf{q}')+\mu_m]^2} -\frac{a^2K_z^2}{4A}\int\frac{d\mathbf{q}'}{(2\pi)^2}\int\frac{d\mathbf{q}''}{(2\pi)^2}N_B\Big(\frac{\epsilon(\mathbf{q}')-\mu_m}{k_BT_m}\Big)N_B\Big(\frac{\epsilon(\mathbf{q}'')-\mu_m}{k_BT_m}\Big)\frac{\mathcal{P}}{\mathbf{q}'\cdot\mathbf{q}''}, \tag{17}$$

where $N_B(x)=[e^x-1]^{-1}$ is the Bose distribution function and $\mathcal{P}$ denotes the principal value of the integral. In Eq. (17) we note that first term on the right-hand side represents the interference between magnons and electrons. This can be seen in Figs. 3(a) and 3(b) where magnons, and thus their interactions, are dressed by their coupling with electrons. Its evaluation is carried out using the result given in Eqs. (13) and (14). Additionally, the second term corresponds to the usual shift of the energy due to the two-particle interaction. To obtain Eq. (17) it has been assumed that the momentum $\hbar\mathbf{q}$ is much smaller than the thermal momenta $\hbar/\Lambda_{\rm th}$ [58], with $\Lambda_{\rm th}=\sqrt{4\pi A/k_BT_m}$ the thermal de Broglie wavelength for the magnons.

When the energy of the single-particle state $\epsilon'(\mathbf{q}\to\mathbf{0})$ becomes less than $\mu_m-a^2K_zn_{\rm th}$, the magnon system becomes unstable. This signals the formation of a magnon Bose-Einstein condensate, a precessional instability, or magnetization reversal. The criterion for such an instability is thus

$$\epsilon'(\mathbf{q}\to\mathbf{0})+a^2K_zn_{\rm th}-\mu_m<0. \tag{18}$$

Based on this condition, a phase diagram is determined in the next section. It is worthwhile to comment that Eq. (18) involves self-consistent physical quantities such as the magnon energy, Eq. (16), magnon temperature, and chemical potential. Unlike previous works [23,42], all these quantities can be evaluated self-consistently at leading order in the interfacial coupling J with the electrons as we outline below. Before proceeding to evaluate Eq. (18), however, we need to determine the magnon chemical potential and temperature for a given electron spin accumulation and temperature. This is done through the Boltzmann equation for magnons with the metallic coupling acting as an electronic reservoir that transfers spin and energy. Details of this calculation are outlined in Appendix E. A Gilbert damping constant α, parametrizing the coupling with phonons, is phenomenologically added. Finally, a steady state is required in the kinetic equations for the total density of magnons and total energy. In this limit, we find relations at thermodynamic equilibrium for the magnon temperature T_m and chemical potential μ_m in terms of the temperature T_e and spin accumulation $\Delta\mu$ of the electrons. These read

$$(1+\chi){\rm Li}_2(z)+\frac{\epsilon_0(\chi-\bar\mu)-\Delta\mu}{k_BT_m}{\rm Li}_1(z)=\frac{\bar\zeta\epsilon_0T_e}{k_BT_m^2}, \tag{19}$$

$$\frac{1+\chi}{2}{\rm Li}_3(z)+\frac{\epsilon_0(2\chi-\bar\mu)-\Delta\mu}{k_BT_m}{\rm Li}_2(z) +\frac{\epsilon_0[\epsilon_0(\chi+\bar\mu)-\Delta\mu]}{k_B^2T_m^2}{\rm Li}_1(z)=\frac{\bar\zeta^2\epsilon_0^2T_e}{6k_B^2T_m^3}, \tag{20}$$

where we used the PolyLogarithm function ${\rm Li}_s(z)=\Gamma^{-1}(s)\int_0^\infty dy y^{s-1}/(e^yz^{-1}-1)$, with $\Gamma(s)$ the gamma function

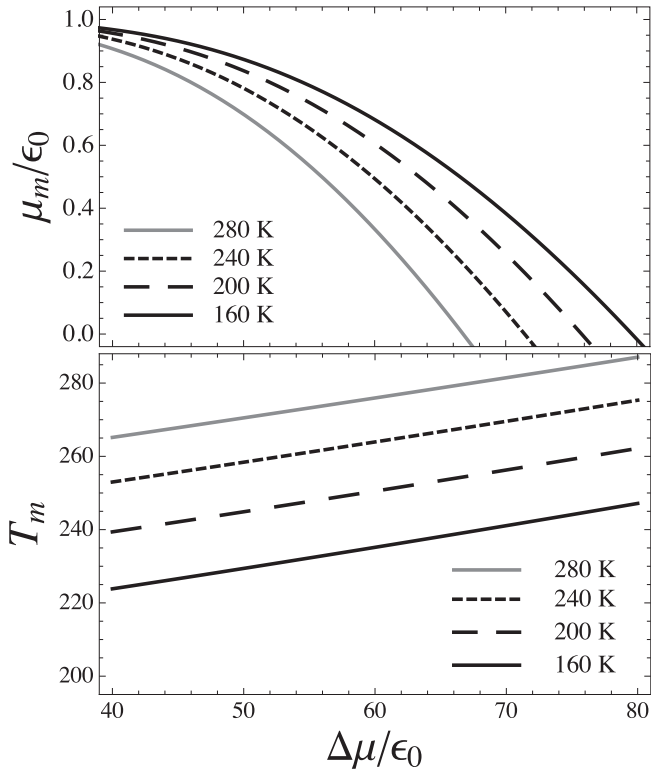

FIG. 4. Chemical potential (top panel) and temperature of magnons (bottom panel) in the steady state as a function of spin accumulation. The plots are displayed for different values of the temperature of the electrons.

and $z = e^{(\mu_m-\epsilon_0)/k_BT_m}$. Equations (19) and (20), are solved for the quantities $\mu_m = \mu_m(\Delta\mu, T_e)$ and $T_m = T_m(\Delta\mu, T_e)$, with the following dimensionless parameters: $\chi = 8\alpha\epsilon_F/k_FSJ^2N(0)a^4$, $\bar{\mu} = (\mu_m - \epsilon_0)/\epsilon_0$, and $\bar{\zeta} = 8Ak_F^2/\epsilon_0$, under consideration.

The steady-state result for μ_m and T_m is shown in Fig. 4 as a function of spin accumulation and various temperatures T_e. These plots were determined for typical values of physical parameters, namely $\epsilon_0 \approx 50$ μeV, $S = 1$, and $\alpha = 10^{-5}$. Through the standard value for the spin-mixing conductance in the YIG|Pt interface, $g^{\uparrow\downarrow} = 10^{14}$ cm^{-2} [14,60], we estimate the interfacial exchange coupling to be $J \approx 50$ meV [60].

IV. CONDENSED AND NORMAL PHASES OF THE MAGNON GAS

In order to obtain results, we evaluate the instability criterion in Eq. (18). To do so, we first rewrite this equation in the dimensionless form

$$\frac{\epsilon'(\mathbf{q}\to\mathbf{0}) + a^2K_zn_{\rm th} - \mu_m}{[JN(0)a^3]k_BT_e} \equiv F[\delta\mu, \eta]. \tag{21}$$

Here $\delta\mu = (\Delta\mu + \mu_m - \epsilon_0)/k_BT_e$ represents the effective chemical potential and $\eta = T_m/T_e$ is the ratio between magnons and electrons temperature. Thus, a simplified expression for the instability criterion is obtained via $F[\delta\mu, \eta] = e_0 + e_1\eta^{3/2} - e_2\delta\mu N_B(-\delta\mu) - \delta\mu$. The coefficients e_0, e_1, and e_2 are dimensionless parameters that obey

$$e_0 = \frac{\epsilon_0 - \mu_m}{k_BT_e}\left(\frac{1}{JN(0)a^3} - 1\right) + \frac{2JS}{k_BT_e} - \frac{K_z^2}{4aAk_BT_eJN(0)} \times \int \frac{d\mathbf{q}'}{(2\pi)^2}\int \frac{d\mathbf{q}''}{(2\pi)^2}N_B\left(\frac{\epsilon(\mathbf{q}') - \mu_m}{k_BT_m}\right) \times N_B\left(\frac{\epsilon(\mathbf{q}'') - \mu_m}{k_BT_m}\right)\frac{\mathcal{P}}{\mathbf{q}'\cdot\mathbf{q}''}, \tag{22}$$

$$e_1 = \left[\frac{\zeta(3/2)}{(4\pi)^{3/2}}\right]\left(\frac{k_BT_e}{A}\right)^{1/2}\frac{K_zd_{\rm F}}{AJN(0)a}, \tag{23}$$

$$e_2 = \frac{a^3k_FK_zJS}{2\epsilon_0\epsilon_F}\int\frac{d\mathbf{q}'}{(2\pi)^2}\mathcal{P}\frac{\ln\left[\frac{1+\sqrt{1-(q'/2k_F)^2}}{q'/2k_F}\right]}{(1-\epsilon(\mathbf{q}')/\epsilon_0)^2}. \tag{24}$$

These parameters show the effect from interfacial coupling, magnon-magnon interactions, and thermal cloud on the magnon gap. Note that e_2 is proportional to the magnon-magnon interaction K_z and the magnon-electron coupling J, thus representing the interference between magnons and electrons. In fact, the two-particle interaction occurs between magnons that are dressed by their coupling with electrons. Taking $\epsilon_0 \sim K_z$ and the critical temperature of the F $T_c \sim A/a^2k_B \ll T_e$ we estimate the dimensionless parameters as $e_0 \sim [1 - (\frac{K_z}{A/a^2S})](\frac{K_z}{k_BT_e})(\frac{\epsilon_F}{J})$, $e_1 \sim (\frac{T_e}{T_c})^{1/2}(\frac{K_z}{k_BT_c})(\frac{\epsilon_F}{J})(\frac{d_F}{a})$, and $e_2 \sim (\frac{J}{\epsilon_F})$. For typical values we expect $e_2 \ll 1$, $e_0 = \mathcal{O}(1)$, but that e_1 can be rather large.

The phase diagram is shown in Fig. 5 as a function of the effective chemical potential $\delta\mu$ and thermal imbalance η, respectively. It consists of a stable and unstable magnon phase, separated by the line $F[\delta\mu, \eta] = 0$, for different values of e_2 [panel (a)] and e_1 [panel (b)]. It is worthwhile to note that in the limit $e_2 \ll 1$, i.e., for $J \ll \epsilon_F$, the criterion for instability reduces to that for a Bose-Einstein condensation in a Bose gas in the Popov approximation [59], for which the critical temperature is $\propto(\delta\mu - e_0)^{2/3}$. On the other hand, the unstable region diminishes as we increase both parameters e_1 and e_2. In particular, when $e_2 > 1$ the unstable region is suppressed. This can be further analyzed by taking the limit $\eta \to 0$ in Eq. (21), where we see that $F \to e_0 + (e_2 - 1)\delta\mu$, for large $\delta\mu$. Clearly, when $e_2 > 1$ the magnon gas never shows an instability if $e_0 > 0$. The term proportional to e_2 stems from combined effects of magnon-electron coupling and magnon-magnon interactions. We thus find that if these combined effects are sufficiently strong, an instability does not occur. While our perturbative approach is not valid in this regime, it still hints at interesting strong-coupling effects. Finally, we remark that at zero spin accumulation, e_0 and e_2 reflect the shift in the energy of single-particle ground state due to the electron-magnon coupling.

V. DISCUSSION AND CONCLUSIONS

In this paper, we have presented a formalism to microscopically investigate how spin currents across a $F|M$ interface lead to instabilities in the magnetic insulator. Our study has

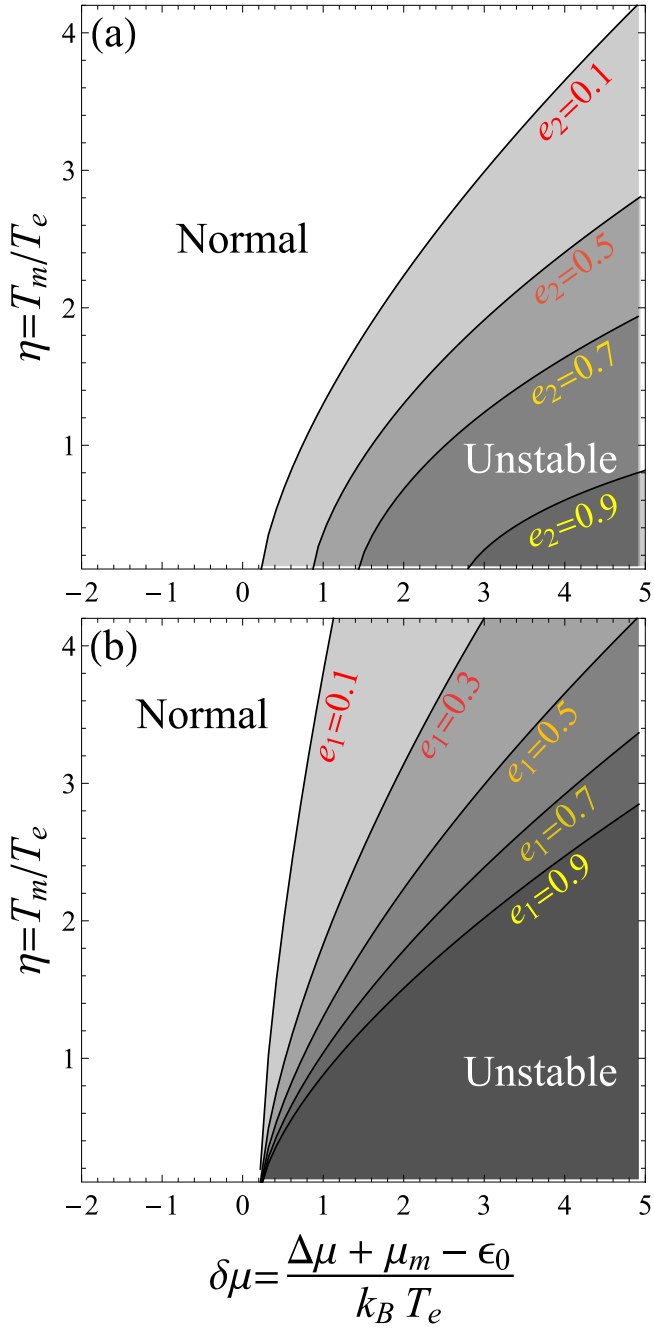

FIG. 5. Phase diagram for the stability of a driven magnon system as a function of the thermal imbalance η and effective chemical potential $\delta\mu$ in units of the thermal energy $k_B T_e$. Each curve delimits both phases, being the right-hand side of the graph where the condition Eq. (18) is fulfilled and thus corresponding to the unstable phase of magnons. In panel (a) we have $e_0 = 0.1$, $e_1 = 0.5$, and $e_2 = 0.1 - 0.9$. Meanwhile, in panel (b) $e_0 = 0.1$, $e_2 = 0.1$, and $e_1 = 0.1 - 0.9$.

been based on a minimal microscopic model for the electrons and magnons in the magnetic insulator, and their coupling. While a direct connection between our results and experiments might be hard to establish, we do find that strong electron-magnon coupling and magnon-magnon interactions may prevent instabilities from occurring. This finding may be of relevance once interfacial electron-magnon interactions are being experimentally explored beyond the YIG-Pt paradigm.

Here, we have investigated electron-magnon and magnon-magnon interactions perturbatively. Future work should address the effects of strong interactions also by other means, i.e., by using the renormalization group. Another interesting direction is extending our theory beyond the linear stability analysis performed here to include the description of the dynamics in the unstable region of the phase diagram.

ACKNOWLEDGMENTS

It is a pleasure to thank S. Bender, Y. Tserkovnyak, and A. S. Nuñez for fruitful discussions. This work was supported by the Netherlands Organization for Scientific Research (NWO), the European Research Council (ERC), and the Research Council of Norway through is Centres of Excellence funding scheme, Project No. 262633, "QuSpin."

APPENDIX A: MAGNON-MAGNON INTERACTION

Here we provide the exact expression for the interacting Hamiltonian of magnons. This is obtained by introducing the Holstein-Primakoff bosons approximated up to order $1/\sqrt{S}$; $\hat{S}^+_{\mathbf{x}} \approx \sqrt{2S}\hat{b}_{\mathbf{x}} - (2\sqrt{2S})^{-1}\hat{b}^\dagger_{\mathbf{x}}\hat{b}_{\mathbf{x}}\hat{b}_{\mathbf{x}}$, $\hat{S}^-_{\mathbf{x}} \approx \sqrt{2S}\hat{b}^\dagger_{\mathbf{x}} - (2\sqrt{2S})^{-1}\hat{b}^\dagger_{\mathbf{x}}\hat{b}^\dagger_{\mathbf{x}}\hat{b}_{\mathbf{x}}$, and $\hat{S}^z_{\mathbf{x}} = (S - \hat{b}^\dagger_{\mathbf{x}}\hat{b}_{\mathbf{x}})$. Then we expand up to fourth order in magnon operators on the spin Hamiltonian Eq. (1). Thus in momentum space the strength of interaction obeys

$$V^{(2,2)}_{\mathbf{q}_1,\mathbf{q}_2,\mathbf{q}_3,\mathbf{q}_4} = \left[\frac{J_e z}{4N}\left(\gamma_{\mathbf{q}_1} + \gamma_{-\mathbf{q}_2} + \gamma_{-\mathbf{q}_3} + \gamma_{\mathbf{q}_4} - 4\gamma_{\mathbf{q}_4-\mathbf{q}_2}\right) + \frac{K_z}{2N}\right] \times \delta_{\mathbf{q}_1+\mathbf{q}_2-\mathbf{q}_3-\mathbf{q}_4}, \tag{A1}$$

where N is the number of spins and $\gamma_{\mathbf{q}} = z^{-1}\sum_\delta e^{\mathbf{q}\cdot\delta}$, with z the coordination number and the sum runs is over next-nearest neighbours. In the long-wavelength limit ($\mathbf{q} \to \mathbf{0}$) the strength of interactions becomes independent on the exchange coupling, $V^{(2,2)}_{\mathbf{q}_1,\mathbf{q}_2,\mathbf{q}_3,\mathbf{q}_4} = (K_z/2N)\delta_{\mathbf{q}_1+\mathbf{q}_2-\mathbf{q}_3-\mathbf{q}_4}$.

APPENDIX B: DERIVATION OF EFFECTIVE ACTION $\mathcal{S}_m[\phi, \phi^*]$ (Eq. (12))

In this section we derive the effective action given in Eq. (12) from Eq. (7). To start with, we consider explicitly the generating functional [Eq. (6)] as

$$\begin{aligned}\mathcal{Z} &= \int \mathcal{D}\phi^*\mathcal{D}\phi\mathcal{D}\psi^*\mathcal{D}\psi \exp\left\{\frac{i}{\hbar}\mathcal{S}_0[\phi,\phi^*] \right. \\ &\quad \left. + \frac{i}{\hbar}\int_{\mathcal{C}^\infty} dt dt' \sum_{\mathbf{x}\mathbf{x}'}\sum_{\sigma\sigma'} \psi^*_{\mathbf{x},\sigma}(t)\mathcal{K}^{\mathbf{x}\mathbf{x}'}_{\sigma\sigma'}(t,t')\psi_{\mathbf{x}',\sigma'}(t')\right\} \\ &= \int \mathcal{D}\phi^*\mathcal{D}\phi\mathcal{D}\exp\left\{\frac{i}{\hbar}\mathcal{S}_0[\phi,\phi^*]\right\}\det\left[-\frac{i}{\hbar}\mathcal{K}\right],\end{aligned} \tag{B1}$$

where $\mathcal{K} = G^{-1} - \delta\mathcal{K}$ is the Kernel defined in Eq. (9). Next, we use the identity $\det[\mathbb{A}] = \exp\{\mathrm{Tr}[\mathrm{Log}(\mathbb{A})]\}$ to expand Eq. (B1) in powers of $\delta\mathcal{K}$. Approximating up to second order

in the electron-magnon coupling we obtain

$$\det[\mathcal{K}] = \exp\{\mathrm{Tr}[\ln(G^{-1} - \delta\mathcal{K})]\} \approx \exp\left\{\mathrm{Tr}[\ln G^{-1}] - \frac{1}{\hbar}\mathrm{Tr}[G\delta\mathcal{K}] - \frac{1}{2\hbar^2}\mathrm{Tr}[G\delta\mathcal{K}G\delta\mathcal{K}]\right\}, \quad \text{(B2)}$$

where in the second line we have used Eq. (10). The two last terms on the right-hand side of Eq. (B2) can be explicitly written as

$$\mathrm{Tr}[G\delta\mathcal{K}] = \int_{\mathcal{C}^\infty} dt dt' \sum_{\mathbf{x}\mathbf{x}'} \sum_{\sigma} G_{\mathbf{x}\mathbf{x}';\sigma\sigma}(t,t')\delta\mathcal{K}^{\mathbf{x}'\mathbf{x}}_{\sigma\sigma}(t',t) \quad \text{(B3)}$$

and

$$\mathrm{Tr}[G\delta\mathcal{K}G\delta\mathcal{K}] = \int_{\mathcal{C}^\infty} dt dt_1 dt_2 dt_3 \sum_{\mathbf{x}\mathbf{x}_1\mathbf{x}_2\mathbf{x}_3} \sum_{\sigma\sigma'} G_{\mathbf{x}\mathbf{x}_1;\sigma\sigma}(t,t_1) \times \delta\mathcal{K}^{\mathbf{x}_1\mathbf{x}_2}_{\sigma\sigma'}(t_1,t_2) G_{\mathbf{x}_2\mathbf{x}_3;\sigma'\sigma'}(t_2,t_3)\delta\mathcal{K}^{\mathbf{x}_3\mathbf{x}}_{\sigma'\sigma}(t_3,t). \quad \text{(B4)}$$

Using the definition for $\delta\mathcal{K}$ given by Eq. (11) we rewrite the sum of Eqs. (B3) and (B4) as

$$\frac{1}{\hbar}\mathrm{Tr}[G\delta\mathcal{K}] + \frac{1}{2\hbar^2}\mathrm{Tr}[G\delta\mathcal{K}G\delta\mathcal{K}] = \frac{i}{\hbar}\int_{\mathcal{C}^\infty} dt dt' \sum_{\mathbf{x}\mathbf{x}'} \phi^*_{\mathbf{x}}(t)\hbar\Sigma_{\mathrm{st};\mathbf{x}\mathbf{x}'}(t,t')\phi_{\mathbf{x}'}(t'), \quad \text{(B5)}$$

with the self-energy defined by Eq. (13). Note that linear, cubic contributions and quartic in ϕ do not appear in Eq. (B5). The first two terms involve non-spin-conserving processes, e.g., like those induced by spin-orbit coupling, which are not considered in the model. Quartic terms in ϕ are nonzero but their contribution at low temperatures becomes negligible with corrections being of the order of $\mathcal{O}[\Delta\mu/(k_B T_e)^2]$.

APPENDIX C: MAGNON SELF-ENERGY DUE TO COUPLING WITH ELECTRONS

In this Appendix, we evaluate the self-energy of the magnons due to their coupling with electrons. We start out with some general remarks for functions on the Keldysh contour.

A function $F(t,t')$, whose arguments are defined on the Keldysh contour, can be decomposed into analytic parts by means of

$$F(t,t') = F^{\delta}(t)\delta(t,t') + \Theta(t,t')F^{>}(t,t') + \Theta(t',t)F^{<}(t,t'), \quad \text{(C1)}$$

with $\Theta(t,t')$ the Heaviside step function on the Keldysh contour and $F^{\delta}(t)$ represents a possible δ singularity. The retarded and advanced components of $F(t,t')$ are related to the analytic parts by

$$F^{(\pm)}(t,t') = \pm\Theta[\pm(t,t')][F^{>}(t,t') - F^{<}(t,t')], \quad \text{(C2)}$$

where $\Theta[\pm(t,t')] \equiv \Theta[\pm(t-t')]$. We also have the Keldysh component

$$F^{K}(t,t') = F^{>}(t,t') + F^{<}(t,t') \quad \text{(C3)}$$

that typically is associated to the strength of fluctuations.

Applying the above definitions to Eq. (13), we see that the Fourier transform of the retarded (advanced) electron bubble is

$$\Pi^{\sigma\sigma',(\pm)}(\mathbf{k},\epsilon) = \int \frac{d\epsilon'}{(2\pi\hbar)} \int \frac{d\epsilon''}{(2\pi\hbar)} \sum_{\mathbf{k}''} A_{\mathbf{k}+\mathbf{k}''}(\epsilon')A_{\mathbf{k}''}(\epsilon'') \times \frac{N_F(\epsilon'-\mu_\sigma) - N_F(\epsilon''-\mu_{\sigma'})}{\epsilon'-\epsilon''-\epsilon^{\pm}}, \quad \text{(C4)}$$

where $A_{\mathbf{k}}(\epsilon)$ denotes the spectral function ($\mathbf{k}$ being a three-dimensional wave vector), $N_F(\epsilon) = [e^{\epsilon/k_B T_e} + 1]^{-1}$ the Fermi distribution function, and μ_σ the chemical potential of electrons with spin projection σ. Ignoring electronic lifetime effects, we use $A_{\mathbf{k}}(\epsilon) = 2\pi\hbar\delta(\epsilon - \epsilon_{\mathbf{k}})$ and approximate up to first order in spin accumulation. We then find that in the long-wavelength and small frequency limit the retarded (advanced) and Keldysh components of electron bubble at low temperatures read

$$\Pi^{\uparrow\downarrow,(\pm)}(\mathbf{k},\epsilon) = \frac{1}{2}N(0)a^3\left[\frac{1}{3}\left(\frac{\mathbf{k}}{2k_F}\right)^2 - 1\right] - \frac{N(0)a^3\epsilon\Delta\mu}{16\epsilon_F^2} \times \left[\left(\frac{2k_F}{\mathbf{k}}\right)^2 + 1\right] \pm i\frac{\pi N(0)a^3 k_F}{8\epsilon_F|\mathbf{k}|}(\Delta\mu - |,\epsilon) \times \Theta\left[1 - \left(\frac{|\mathbf{k}|}{2k_F}\right)^2\right] \quad \text{(C5)}$$

and

$$\Pi^{\uparrow\downarrow,K}(\mathbf{k},\epsilon) = -\frac{i\pi N(0)a^3 m k_B T_e}{\hbar^2 k_F|\mathbf{k}|}\Theta\left[1 - \left(\frac{|\mathbf{k}|}{2k_F}\right)^2\right], \quad \text{(C6)}$$

with a the lattice constant, m the mass of electrons, and $N(0) = mk_F/\pi^2\hbar^2$ the electronic density of states at the Fermi level. The imaginary part of the self-energy Eq. (13) represents the rate of change of the number of magnons. From Eq. (14), we see that the evolution of the number of magnons corresponds to the competition between the spin transfer ($\propto\Delta\mu \equiv \mu_\uparrow - \mu_\downarrow$) and spin pumping mechanisms ($\propto\epsilon$). In principle, the magnon-electron coupling matrix element can be determined in terms of the mixing conductance, but this identification will not be pursued here [5,6].

APPENDIX D: LADDER APPROXIMATION

In Sec. III A, we derived an action for the gas of magnons, which are excited by the combined effects of a thermal gradient and the spin-transfer torque across the $F|M$ interface. Here, we discuss more details of this derivation.

We introduce the order parameter $\langle\phi_{\mathbf{q}}(t)\rangle$, that characterizes the instability. This is accomplished by performing a Legendre transformation [61] on the magnon field variables that ultimately leads to an effective action for $\Psi_{\mathbf{q}}(t) \equiv \langle\phi_{\mathbf{q}}(t)\rangle$. With this aim we start out by introducing the

generating functional for Keldysh Green's functions, following Ref. [58], as

$$\mathcal{Z}[J,J^*] = \int \mathcal{D}[\phi^*]\mathcal{D}[\phi] \times \exp\left\{\frac{i}{\hbar}\mathcal{S}_{\rm m}[\phi,\phi^*] + i(J^\alpha\phi_\alpha + {\rm c.c.})\right\}, \quad \text{(D1)}$$

where J_α and J^α are sources that are defined on the Keldysh contour and summation over repeated indices means an integration over space and time coordinates. Then the Legendre transformation [61]

$$\Gamma[\Psi,\Psi^*] \equiv \Psi^\alpha J_\alpha + J^\alpha\Psi_\alpha - W[J,J^*], \quad \text{(D2)}$$

where $W[J,J^*] = -i\ln\mathcal{Z}[J,J^*]$ is the generating functional for connected Green's functions, which can be evaluated in terms of a perturbation series. The order parameter is then $\Psi_\alpha \equiv \delta W/\delta J^\alpha = \langle\phi_\alpha\rangle$. The functional $-\hbar\Gamma[\phi,\phi^*]$, that generates all one-particle irreducible diagrams, corresponds to the effective action. We now do perturbation theory in the interaction to evaluate the effective action in terms of the coefficients $\Gamma^{(2n)}$ (up to $n=2$) of the term that is of order n in the fields. Those coefficients in momentum space correspond to

$$\hbar\Gamma^{(2)}(\mathbf{q};t,t') = -\left[\left(i\hbar\frac{\partial}{\partial t} - \epsilon(\mathbf{q}) + \mu_m\right)\delta(t,t') - \hbar\Sigma_{\rm st}(\mathbf{q};t,t')\right] + \hbar\Sigma_{\rm in}(\mathbf{q};t,t'), \quad \text{(D3)}$$

$$\hbar\Gamma^{(4)}(\mathbf{q},\mathbf{q}',\mathbf{Q};t,t') = T(\mathbf{q},\mathbf{q}',\mathbf{Q};t,t') + T(-\mathbf{q},\mathbf{q}',\mathbf{Q};t,t'), \quad \text{(D4)}$$

where the interacting self-energy $\hbar\Sigma_{\rm in}$ was introduced by the Dyson equation for the magnon Green's function $\mathcal{G} = \mathcal{G}_0 + \mathcal{G}_0\hbar\Sigma_{\rm in}\mathcal{G}$. Here $\mathcal{G}_0$ is the dressed magnon propagator due to the contact with the M; see Fig. 3(a), according to Eq. (13). The two-body interaction is evaluated within the T-matrix (or ladder) approximation [58], diagrammatically indicated in Fig. 3(c), which describes the scattering of two magnons that at time t' have the momenta $\hbar(\mathbf{Q}\pm\mathbf{q}')$ and at time t the momenta $\hbar(\mathbf{Q}\pm\mathbf{q})$. The exact interacting self-energy obeys the relation

$$\hbar\Sigma_{\rm in}(\mathbf{q};t,t') = i\int\frac{d\mathbf{q}'}{(2\pi)^2}\hbar\Gamma^{(4)}(\mathbf{q}-\mathbf{q}',\mathbf{q}-\mathbf{q}',\mathbf{q}+\mathbf{q}';t,t')\mathcal{G}(\mathbf{q}';t',t). \quad \text{(D5)}$$

In Fourier space the expression for the retarded component of the interacting self-energy Eq. (D5) take the form

$$\hbar\Sigma^{(+)}_{\rm in}(\mathbf{q};\epsilon) = i\int\frac{d\mathbf{q}'}{(2\pi)^2}\int\frac{d\epsilon'}{(2\pi)}\Gamma^{(+)}_4(\mathbf{q}-\mathbf{q}',\mathbf{q}-\mathbf{q}',\mathbf{q}+\mathbf{q}';\epsilon+\epsilon')\mathcal{G}^{(+)}(\mathbf{q}';\epsilon')\hbar\Sigma^<_{\rm st}(\mathbf{q}';\epsilon')\mathcal{G}^{(-)}(\mathbf{q}';\epsilon') + i\int\frac{d\mathbf{q}'}{(2\pi)^2}\int\frac{d\epsilon'}{(2\pi)}\Gamma^<_4(\mathbf{q}-\mathbf{q}',\mathbf{q}-\mathbf{q}',\mathbf{q}+\mathbf{q}';\epsilon+\epsilon')\mathcal{G}^{(-)}(\mathbf{q}';\epsilon'). \quad \text{(D6)}$$

The evaluation of Eq. (D6) is carried out by expanding up to second order in the coupling with the leads. In this approach the various components of the Green's function for magnons are approximated by

$$\mathcal{G}^{(\pm)} = \mathcal{G}^{(\pm)}_0 + \mathcal{G}^{(\pm)}_0\hbar\Sigma^{(\pm)}_{\rm st}\mathcal{G}^{(\pm)}_0 + \cdots, \quad \text{(D7)}$$

$$\mathcal{G}^< = \mathcal{G}^{(+)}\hbar\Sigma^<_{\rm st}\mathcal{G}^{(-)} = \mathcal{G}^{(+)}_0\hbar\Sigma^<_{\rm st}\mathcal{G}^{(-)}_0 + \cdots, \quad \text{(D8)}$$

as can be seen in Fig. 3(b). On the other hand, the magnon-magnon interactions will be approximated by a contact interaction, and therefore $\mathrm{T}^{(\pm)}(\mathbf{q},\mathbf{q}',\mathbf{Q};\epsilon) \approx \frac{K_\pm}{2}$. After some manipulations [58], we arrive at the semiclassical effective action Eq. (15), describing the low-energy dynamics of the interacting magnons.

APPENDIX E: SELF-CONSISTENT RELATIONS: CHEMICAL POTENTIALS AND TEMPERATURES

In this section we compute the chemical potential and temperature of magnons assuming that magnons are sufficiently close to equilibrium.

The total spin-current flowing across the interface is quantified by the rate of change of magnons in the F, that may be obtained following standard methods described in Ref. [58]. It consists of analyzing the stochastic dynamics of magnons due to the coupling with the M, that ultimately turns out in a Boltzmann equation. For this purpose we split the magnon field, in Eq. (12), into semiclassical and fluctuating parts according to $\phi_{\mathbf{q}}(t_\pm) = \varphi_{\mathbf{q}}(t) \pm \xi_{\mathbf{q}}(t)/2$, where $t_\pm$ refers to the forward and backward branches of the Keldysh contour, respectively, and $\xi_{\mathbf{q}}(t)$ the fluctuations. After integrating out the fluctuations $\xi_{\mathbf{q}}(t)$ in the action, Eq. (12), we find that the field $\varphi_{\mathbf{q}}(t)$ obeys the Langevin equations

$$i\hbar\frac{\partial}{\partial t}\varphi_{\mathbf{q}}(t) = (\epsilon(\mathbf{q}) - \mu_m)\varphi_{\mathbf{q}}(t) + \int dt'\hbar\Sigma^{(+)}_{\rm st}(\mathbf{q};t,t')\varphi_{\mathbf{q}}(t') + \eta_{\mathbf{q}}(t) \quad \text{(E1)}$$

and

$$-i\hbar\frac{\partial}{\partial t}\varphi^*_{\mathbf{q}}(t) = [\epsilon(\mathbf{q}) - \mu_m]\varphi^*_{\mathbf{q}}(t) + \int dt'\varphi^*_{\mathbf{q}}(t')\hbar\Sigma^{(-)}_{\rm st}(\mathbf{q};t,t') + \eta^*_{\mathbf{q}}(t) \quad \text{(E2)}$$

with the Gaussian stochastic noise $\eta_{\mathbf{q}}(t)$ and $\eta^*_{\mathbf{q}}(t)$ is zero on average and has the correlations

$$\langle\eta_{\mathbf{q}}(t)\eta^*_{\mathbf{q}}(t')\rangle = \frac{i\hbar}{2}\hbar\Sigma^K_{\rm st}(\mathbf{q};t-t'). \quad \text{(E3)}$$

In the low-energy approximation we see that the strength of the noise is evaluated directly from the combination of

Eqs. (13) and (C6). This relation between noise and damping stems from the fluctuation-dissipation theorem [62] and ensures us that the magnon gas relaxes to thermal equilibrium.

Note that to obtain Eqs. (E1) and (E2), as a first step, we have not taken into account the interaction between magnons. However, the collision terms will be included next in the Boltzmann equation. We take into account the leading low-energy contribution of the self-energy, i.e., $\int dt' \hbar\Sigma^{(+)}_{\rm st}(\mathbf{q};t,t')\varphi_{\mathbf{q}}(t') \simeq [\hbar\Sigma^{(+)}_{\rm st}(\mathbf{q},0) + \hbar\Sigma^{(+)\prime}_{\rm st}(\mathbf{q},0) i\hbar\frac{\partial}{\partial t}]\varphi_{\mathbf{q}}(t)$. Finally, the rate equation for the magnons due to the coupling at the interface with the electron reservoir is written explicitly as

$$i\hbar\left(\frac{\partial n(\mathbf{q},t)}{\partial t}\right)\Big|_{\rm st} = 2i{\rm Im}[\hbar\Sigma^{(+)\prime}_{\rm st}(\mathbf{q},0)](\epsilon_{\mathbf{q}}-\mu_m)n(\mathbf{q},t) + 2i{\rm Im}[\hbar\Sigma^{(+)}_{\rm st}(\mathbf{q},0)]n(\mathbf{q},t) - \frac{1}{2}\hbar\Sigma^{K}_{\rm st}(\mathbf{q},0) \tag{E4}$$

with $n(\mathbf{q},t) = \langle\phi^*_{\mathbf{q}}\phi_{\mathbf{q}}\rangle$ and $\langle\dots\rangle$ stand for averaging over noise realization. Therefore, the full dynamics for the distribution of magnons in the F is determined by the Boltzmann equation

$$\frac{\partial n(\mathbf{q},t)}{\partial t} = -2\alpha\omega_{\mathbf{q}}n(\mathbf{q},t) + \left(\frac{\partial n(\mathbf{q},t)}{\partial t}\right)\Big|_{\rm st} \tag{E5}$$

with α the Gilbert damping constant and where the collisions term has been considered. Taking moments of Eq. (E5) we obtain a closed set of equations for the total number of magnons and energy. In equilibrium, there will be neither spin flow nor energy transfer through the interface. This is implemented by requiring $\partial n(t)/\partial t \equiv \frac{\partial}{\partial t}\sum_{\mathbf{q}} n(\mathbf{q},t) = 0$ and $\partial\epsilon(t)/\partial t \equiv \frac{\partial}{\partial t}\sum_{\mathbf{q}}\epsilon_{\mathbf{q}}n(\mathbf{q},t) = 0$, that turn out in the pair of Eqs. (19) and (20).

[1] S. A. Wolf, Science **294**, 1488 (2001).
[2] S. Takahashi and S. Maekawa, Sci. Technol. Adv. Mater. **9**, 014105 (2008).
[3] A. Brataas, A. D. Kent, and H. Ohno, Nat. Mater. **11**, 372 (2012).
[4] I. Žutić, J. Fabian, and S. Das Sarma, Rev. Mod. Phys. **76**, 323 (2004).
[5] Y. Tserkovnyak, A. Brataas, and G. E. W. Bauer, Phys. Rev. Lett. **88**, 117601 (2002).
[6] Y. Tserkovnyak, A. Brataas, G. E. W. Bauer, and B. I. Halperin, Rev. Mod. Phys. **77**, 1375 (2005).
[7] J. Xiao, G. E. W. Bauer, K.-c. Uchida, E. Saitoh, and S. Maekawa, Phys. Rev. B **81**, 214418 (2010).
[8] X. Jia, K. Liu, K. Xia, and G. E. W. Bauer, Europhys. Lett. **96**, 17005 (2011).
[9] J. Xiao and G. E. W. Bauer, Phys. Rev. Lett. **108**, 217204 (2012).
[10] Y.-T. Chen, S. Takahashi, H. Nakayama, M. Althammer, S. T. B. Goennenwein, E. Saitoh, and G. E. W. Bauer, Phys. Rev. B **87**, 144411 (2013).
[11] A. Kapelrud and A. Brataas, Phys. Rev. Lett. **111**, 097602 (2013).
[12] Y. Zhou, H. J. Jiao, Y.-t. Chen, G. E. W. Bauer, and J. Xiao, Phys. Rev. B **88**, 184403 (2013).
[13] S. S.-L. Zhang and S. Zhang, Phys. Rev. B **86**, 214424 (2012).
[14] Y. Kajiwara, K. Harii, S. Takahashi, J. Ohe, K. Uchida, M. Mizuguchi, H. Umezawa, H. Kawai, K. Ando, K. Takanashi, S. Maekawa, and E. Saitoh, Nature (London) **464**, 262 (2010).
[15] C. W. Sandweg, Y. Kajiwara, K. Ando, E. Saitoh, and B. Hillebrands, Appl. Phys. Lett. **97**, 252504 (2010).
[16] C. W. Sandweg, Y. Kajiwara, A. V. Chumak, A. A. Serga, V. I. Vasyuchka, M. B. Jungfleisch, E. Saitoh, and B. Hillebrands, Phys. Rev. Lett. **106**, 216601 (2011).
[17] Z. Wang, Y. Sun, M. Wu, V. Tiberkevich, and A. Slavin, Phys. Rev. Lett. **107**, 146602 (2011).
[18] S. M. Rezende, R. L. Rodríguez-Suárez, M. M. Soares, L. H. Vilela-Leão, D. Ley Domínguez, and A. Azevedo, Appl. Phys. Lett. **102**, 012402 (2013).
[19] H. Nakayama, M. Althammer, Y.-T. Chen, K. Uchida, Y. Kajiwara, D. Kikuchi, T. Ohtani, S. Geprägs, M. Opel, S. Takahashi, R. Gross, G. E. W. Bauer, S. T. B. Goennenwein, and E. Saitoh, Phys. Rev. Lett. **110**, 206601 (2013).
[20] Z. Qiu, K. Ando, K. Uchida, Y. Kajiwara, R. Takahashi, H. Nakayama, T. An, Y. Fujikawa, and E. Saitoh, Appl. Phys. Lett. **103**, 092404 (2013).
[21] L. Berger, Phys. Rev. B **54**, 9353 (1996).
[22] J. Slonczewski, J. Magn. Magn. Mater. **159**, L1 (1996).
[23] S. A. Bender, R. A. Duine, and Y. Tserkovnyak, Phys. Rev. Lett. **108**, 246601 (2012).
[24] A. Hamadeh, O. d'Allivy Kelly, C. Hahn, H. Meley, R. Bernard, A. H. Molpeceres, V. V. Naletov, M. Viret, A. Anane, V. Cros, S. O. Demokritov, J. L. Prieto, M. Muñoz, G. de Loubens, and O. Klein, Phys. Rev. Lett. **113**, 197203 (2014).
[25] C. Safranski, I. Barsukov, H. K. Lee, T. Schneider, A. A. Jara, A. Smith, H. Chang, K. Lenz, J. Lindner, Y. Tserkovnyak, M. Wu, and I. N. Krivorotov, Nat. Commun. **8**, 117 (2017).
[26] M. Schneider, T. Brächer, V. Lauer, P. Pirro, D. A. Bozhko, A. A. Serga, H. Yu. Musiienko-Shmarova, B. Heinz, Q. Wang, T. Meyer, F. Heussner, S. Keller, E. Th. Papaioannou, B. Lägel, T. Löber, V. S. Tiberkevich, A. N. Slavin, C. Dubs, B. Hillebrands, and A. V. Chumak, arXiv:1612.07305.
[27] S. O. Demokritov, V. E. Demidov, O. Dzyapko, G. A. Melkov, A. A. Serga, B. Hillebrands, and A. N. Slavin, Nature (London) **443**, 430 (2006).
[28] S. M. Rezende, Phys. Rev. B **79**, 174411 (2009).
[29] A. I. Bugrij and V. M. Loktev, Low Temp. Phys. **33**, 37 (2007).
[30] A. I. Bugrij and V. M. Loktev, Low Temp. Phys. **34**, 992 (2008).
[31] A. I. Bugrij and V. M. Loktev, Low Temp. Phys. **35**, 770 (2009).
[32] R. E. Troncoso and Á. S. Núñez, J. Phys.: Condens. Matter **24**, 036006 (2011).
[33] F. Li, W. M. Saslow, and V. L. Pokrovsky, Sci. Rep. **3**, 1372 (2013).
[34] R. E. Troncoso and Á. S. Núñez, Ann. Phys. **346**, 182 (2014).
[35] J. P. Eisenstein and A. H. MacDonald, Nature (London) **432**, 691 (2004).
[36] L. V. Butov, J. Phys.: Condens. Matter **16**, R1577 (2004).

[37] T. Fukuzawa, E. E. Mendez, and J. M. Hong, Phys. Rev. Lett. **64**, 3066 (1990).
[38] O. Misochko, M. Hase, K. Ishioka, and M. Kitajima, Phys. Lett. A **321**, 381 (2004).
[39] J. Kasprzak, M. Richard, S. Kundermann, A. Baas, P. Jeambrun, J. M. J. Keeling, F. M. Marchetti, M. H. Szymańska, R. André, J. L. Staehli, V. Savona, P. B. Littlewood, B. Deveaud, and L. S. Dang, Nature (London) **443**, 409 (2006).
[40] J. Klaers, J. Schmitt, F. Vewinger, and M. Weitz, Nature (London) **468**, 545 (2010).
[41] V. V. Kruglyak, S. O. Demokritov, and D. Grundler, J. Phys. D **43**, 264001 (2010).
[42] S. A. Bender, R. A. Duine, A. Brataas, and Y. Tserkovnyak, Phys. Rev. B **90**, 094409 (2014).
[43] S. Maekawa, S. O. Valenzuela, E. Saitoh, and T. Kimura, *Spin Current* (Oxford University Press, Oxford, UK, 2017).
[44] L. J. Cornelissen, K. J. H. Peters, G. E. W. Bauer, R. A. Duine, and B. J. van Wees, Phys. Rev. B **94**, 014412 (2016).
[45] C. Du, T. van der Sar, T. X. Zhou, P. Upadhyaya, F. Casola, H. Zhang, M. C. Onbasli, C. A. Ross, R. L. Walsworth, Y. Tserkovnyak, and A. Yacoby, Science **357**, 195 (2017).
[46] T. Holstein and H. Primakoff, Phys. Rev. **58**, 1098 (1940).
[47] A. I. Akhiezer and S. V. Peletminskiii, *Spin Waves* (North-Holland Pub. Co., Amsterdam, 1968).
[48] A. Auerbach, *Interacting Electrons and Quantum Magnetism* (Springer-Verlag, New York, 1994).
[49] L. C. Davis and S. H. Liu, Phys. Rev. **163**, 503 (1967).
[50] R. B. Woolsey and R. M. White, Phys. Rev. B **1**, 4474 (1970).
[51] J. A. Hertz and D. M. Edwards, J. Phys. F **3**, 2174 (1973).
[52] D. K. Singh and A. Singh, Phys. Rev. B **88**, 144410 (2013).
[53] F. Mahfouzi and B. K. Nikolić, Phys. Rev. B **90**, 045115 (2014).
[54] Y. Ohnuma, M. Matsuo, and S. Maekawa, Phys. Rev. B **94**, 184405 (2016).
[55] A. Kamra and W. Belzig, Phys. Rev. B **94**, 014419 (2016).
[56] N. Rohling, E. L. Fjærbu, and A. Brataas, Phys. Rev. B **97**, 115401 (2018).
[57] J. Zheng, S. Bender, J. Armaitis, R. E. Troncoso, and R. A. Duine, Phys. Rev. B **96**, 174422 (2017).
[58] H. T. C. Stoof, J. Low Temp. Phys. **114**, 11 (1999).
[59] L. P. Pitaevskii and S. Stringari, *Bose-Einstein Condensation* (Clarendon, Oxford, 2003).
[60] B. Heinrich, C. Burrowes, E. Montoya, B. Kardasz, E. Girt, Y.-Y. Song, Y. Sun, and M. Wu, Phys. Rev. Lett. **107**, 066604 (2011).
[61] D. J. Amit, *Field Theory: The Renormalization Group and Critical Phenomena* (World Scientific, Singapore, 1984).
[62] L. P. Kadanoff and G. Baym, *Quantum Statistical Mechanics: Green's Function Methods in Equilibrium and Nonequilibrium Problems* (Addison-Wesley, New York, 1962).